Metal Decoration of TiO_2 Nanotubes for Photocatalytic and Water Splitting Applications

Gisele Inês Selli, Maria Luisa Puga and Fernando Bonatto

Abstract TiO_2 materials, especially nanostructures, must not only be cost-effective, but they must also meet many other requirements: high photocatalytic activity, large active superficial area, chemical resistance, ease of manufacture, and fast synthesis route. However, it is commonly recurrent that TiO_2 nanostructures, nanoparticles or nanotubes, still have a high deficiency to collect a large part of the light spectrum. Nevertheless, anatase/rutile superficial defects, which increases considerably charge carrier recombination, can be circumvented by the addition of transition/noble metals, to intentionally increase the material photocatalytic properties and extend applications, in the field of H_2 generation.

Keywords TiO_2 · Photocatalysis · H_2 production · Metal decoration

Abbreviations

AO7	Acid Orange 7
BET	Brunauer–Emmett–Teller
EDX	Energy Dispersive X-ray
FESEM	Field Emission Scanning Electron Microscopy
FT-IR	Fourier Transformer Infrared
MB	Methylene Blue
PO	Heterogeneous Photocatalytic Oxidation
TNT	Titanium dioxide Nanotubes

G. I. Selli (✉) · M. L. Puga · F. Bonatto
Universidade Federal do Rio Grande do Sul, Porto Alegre, Brazil
e-mail: gisele.selli@ufrgs.br

F. Bonatto
e-mail: bonatto02@yahoo.com.br

A. Kopp Alves (ed.), *Nanomaterials for Eco-friendly Applications*,
Engineering Materials, https://doi.org/10.1007/978-3-030-26810-7_5

1 Introduction

With the advent of industries that produce a large number of pollutants in effluents, including pharmaceuticals, textiles, and chemicals, the amount of pollutants has grown almost exponentially in the last 30 years according to the UN survey in 2018. For this reason, in the context of reducing the number of emerging pollutants in industrial effluents. In this idea, titanium dioxide has become a highly researched material with high potential for commercial and industrial applicability. However, one of the major drawbacks is the fact that the material has a gap within the UV light spectrum and is considered a high bandgap semiconductor, which restricts its applications. Although this characteristic represents a depreciation of the material, since this part of the spectrum is smaller when compared to the whole spectrum available, the fact that the TiO_2 is low cost, with high physical-chemical stability and easy to manufacture makes it an attractive material for photocatalytic applications.

To increase the industrial use and applicability of nanostructured TiO_2, as a base element in the decomposition of pollutants, processes such as doping and decoration are widely used because of the ease of synthesis in conjunction with titanium dioxide. One of the most successful approaches is the use of transition and noble metals together with TiO_2 nanostructures. In addition to allowing access to a more significant portion of the available light spectrum, thereby increasing the photocatalytic activity, the presence of these metals still allows an improvement of yield and applicability in the decomposition of different chemical compounds present in effluents. This chapter presents a condensation of the primary metals used together with TiO_2.

This chapter aims to show the latest advances in the application of photocatalytic processes for the decomposition of pollutants and H_2 production using metals such as Fe, Cu, Ag, and Au together with TiO_2 nanostructures for their simplicity of synthesis and low cost for direct application.

2 Iron-Doped TiO_2

Although having wide application potential, titanium dioxide nanotubes (TNTs) face a major drawback regarding their large band gap, an aspect that limits photoresponse almost exclusively to the ultraviolet region [1]. Modifying TiO_2 with other narrow bandgap materials is a widely recognized method to minimize such drawback, as it causes a red shift of the absorption edge to the visible light region [2–4]. Moreover, selective metal ion doping, especially iron in its Fe^{3+} form [5, 6], significantly broadens light response range and inhibits charge-carrier recombination as the ions act as charge traps for the photogenerated electron-hole pairs [7–11]. Several studies also pointed out to an enhanced photocatalytic activity for Fe-doped catalysts both under UV [11–13] and visible light irradiation [14–17]. As demonstrated by Yu et al. [18], such high performance of Fe^{3+}/TiO_2 is attributed to the accumulation of photogen-

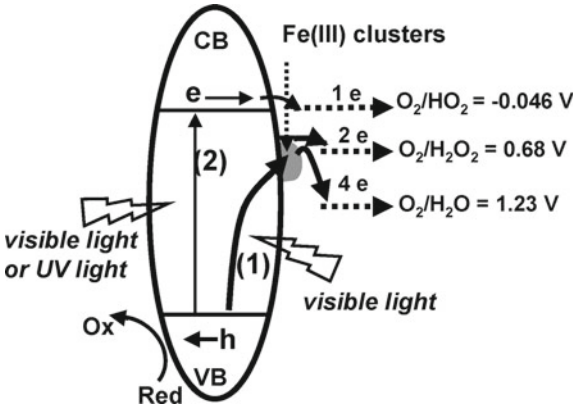

Fig. 1 Schematic diagram illustrating the possible photocatalytic mechanism of Fe^{3+}/TiO_2, involving interfacial charge transfer (arrow 1) and multielectron reduction processes. The band gap excitation is indicated by arrow 2. Reprinted with permission [18]

erated holes in the valence band (VB) of TiO_2 and the catalytic reduction of oxygen by photoreduced Fe^{2+} species on TiO_2 surface (Fig. 1).

Regarding Fe/TNTs, Asiltürk et al. [19] found that Fe^{3+} doping may prevent particle agglomeration due to the formation of well-defined crystalline nanoparticles (NPs) with high surface area, two key aspects to improving photocatalytic performance [19]. Compared to undoped, electrochemically anodized TNTs, Fe^{3+} doped nanotubes have shown a six-fold increase on photocurrent density and a doubled degradation rate measurement [1]. Using the crystal structure of TiO_2 as a matrix for fixating Fe^{3+} NPs is also presented as an alternative to having them dispersed in an aqueous suspension, thus avoiding the detrimental nanoparticle aggregation where many particles are hidden from light absorption [5].

Fe_2O_3 has been pointed out as another strong candidate for being a low cost, nontoxic and highly stable form of iron oxide [20, 21]. Concerning morphology, aggregating Fe NPs in adequate amounts to TNTs does not affect the highly ordered nanotube construction, as demonstrated by Zhang et al. [1] in Fig. 2, where SEM images compare undoped two-step anodized TiO_2 NTs with Fe^{3+}-doped TiO_2 NTs, also fabricated via a two-step anodization process. Xie et al. [22] reinforce this conclusion by successfully electrodepositing $ZnFe_2O_4$ nanoparticles within self-organized and highly ordered TiO_2 nanotube arrays while minimizing the clogging of the tube entrances (Fig. 3).

Cong et al. [23] studied the performance of α-Fe_2O_3/TNTs composites for photoelectro-Fenton degradation using phenol, a compound usually found in wastewater discharged from a variety of industries [24, 25], as a model pollutant with an initial concentration of 10 mg/L. The α-Fe_2O_3/TNT complex was synthesized over anodized nanotubes by two different techniques, a dipping method in aqueous suspension of α-Fe_2O_3 NPs (fixed-Fe_2O_3 system 1) and an electrochemical deposition (fixed-Fe_2O_3 system 2), for which the electrodes fabricated via the second one pre-

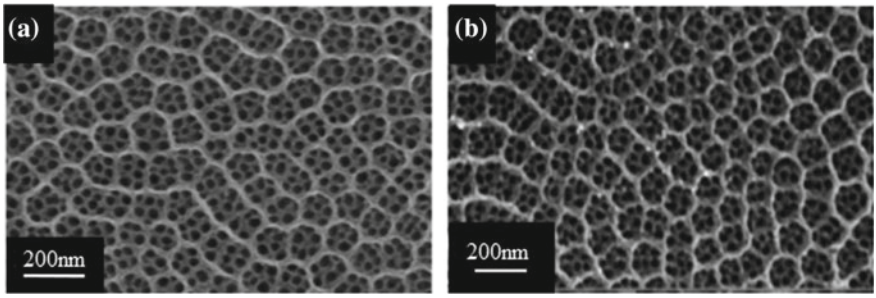

Fig. 2 SEM images of: **a** TiO_2 NTs in the two-step anodization. **b** Fe^{3+}/TiO_2 NTs. Reprinted with permission [1]

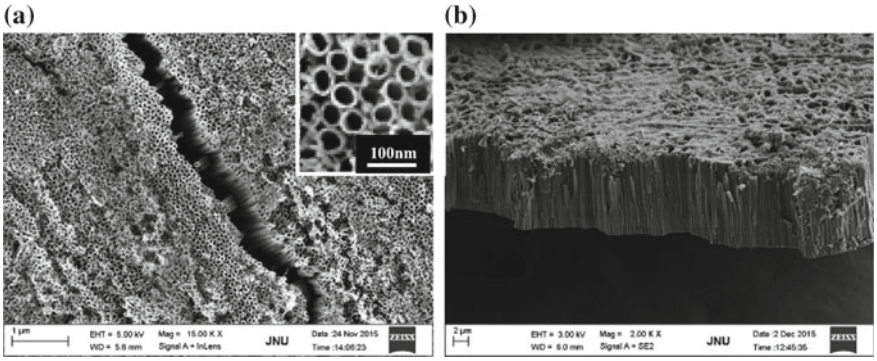

Fig. 3 **a** Top-view and **b** side-view SEM images of the TiO_2 nanotube arrays. The inset shows the images of TNTs at high magnification. Reprinted with permission [22]

sented higher removal efficiency of phenol and stronger photoresponse under visible light irradiation due to the uniform fixation of Fe NPs on TNTs. To further investigate the role of α-Fe_2O_3 NPs, phenol degradation was also carried in a dispersed system, where α-Fe_2O_3 NPs were added into the aqueous phenol solution instead of being attached to TNT electrodes. Responses to three different Fenton-related processes, electro-Fenton, visible light photoelectro-Fenton, and UV-visible light photoelectro-Fenton, are depicted in Fig. 4. After a 60 min treatment, electrochemically deposited α-Fe_2O_3/TNT electrodes presented 100% phenol removal efficiency in the UV-visible light photoelectro-Fenton process, whereas the dispersed system required double the amount of time to reach similar rates. The increased performance of Fe_2O_3 modified TNTs could be linked to the fact that incorporating α-Fe_2O_3 NPs effectively suppressed the recombination of electron-hole pairs, thus allowing them to act as heterogeneous catalysts for phenol degradation [23].

$ZnFe_2O_4$ appears as an opportunity to harvest most of the visible portion of the solar spectrum [26], also presenting an alternative to overcome the separation and recycling process of the powdered $ZnFe_2O_4$ and improving the energy conversion

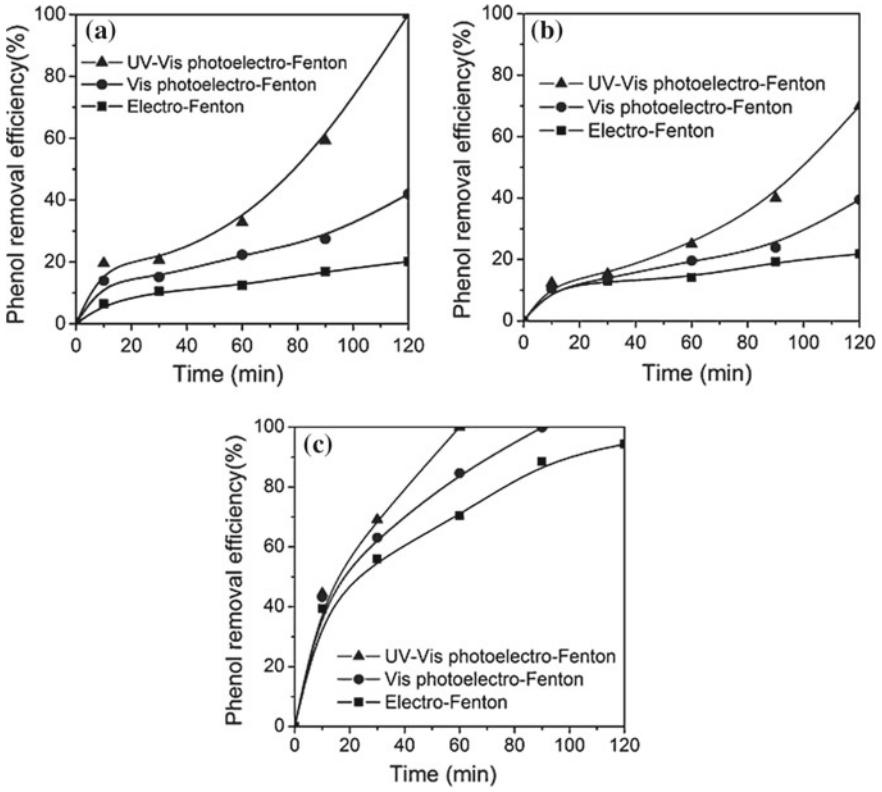

Fig. 4 Phenol degradation in **a** dispersed system, **b** fixed-Fe_2O_3 system 1, and **c** fixed-Fe_2O_3 system 2. Reprinted with permission [23]

efficiency when aggregated to TiO_2 in a $ZnFe_2O_4$/TNT composite [27]. Loading highly ordered TiO_2 nanotube arrays with $ZnFe_2O_4$ NPs enhances absorption in both UV and visible light regions promotes greater separation of photoinduced electron-hole pairs and presents a more effective photoconversion capability than undoped TNTs [22, 27]. Moreover, Xie et al. [22] demonstrated that the photocurrent density of the composite $ZnFe_2O_4$/TNT (Z-TNT) electrode was more than 5.5 times higher than that of the TNT electrode alone (Fig. 5), implying that $ZnFe_2O_4$ can be effectively used to sensitize TiO_2 nanotube array electrodes. Regarding its applicability, the synthesized electrode was found to possess excellent photoelectro-catalytic activity for degradation of 4-chlorophenol, a toxic and non-biodegradable pollutant present in wastewater of industrial activities [28, 29] under UV light illumination, presenting 100% efficiency with an applied potential bias of 0.8 V, 16% higher than the degradation efficiency measured for the unloaded TNT electrode [27].

Titanium nanotube composites are also attractive photocatalysts for photoelectrochemical (PEC) solar water splitting applications due to their high-efficiency energy conversion, good chemical stability, and corrosion resistance in aqueous envi-

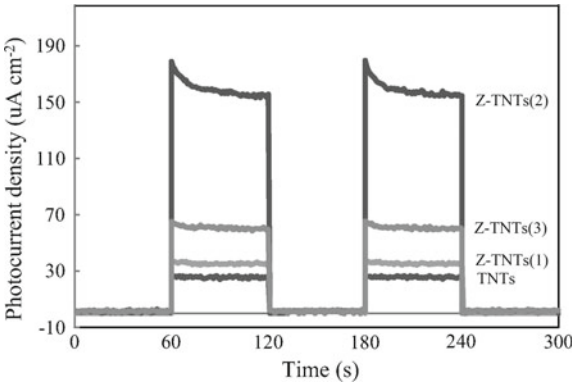

Fig. 5 **a** Transient photocurrent responses of the TNTs and the Z-TNTs samples under the bias potential of 0.8 V versus SCE. Three $ZnFe_2O_4$/TNT samples were analyzed, each containing a distinct concentration of $Fe(NO_3)_3$ and $Zn(NO_3)_2$: (1) 0.5 M and 0.25 M; (2) 1.0 M and 0.5 M; (3) 2.0 M and 1.0 M, respectively. Reprinted with permission [22]

ronments [30–33]. PEC splitting of water is an ideal, low-cost renewable method of hydrogen (H_2) production that integrates solar energy collection and water electrolysis in a single photocell [30, 34, 35]. Figure 6 presents the principle of photocatalytic water splitting reactions.

Moreover, H_2 has been considered an attractive energy carrier, achieving much higher conversion efficiency than the conventional fossil fuels, while offering a more sustainable [33], environmentally benign energy source with lesser emissions [36]. Unfortunately, large-scale application of most photocatalytic systems is restricted by the fact that noble metal-based co-catalysts are still the first option for achieving reasonable activity rates. Therefore, seeking cheap, earth-abundant and high-performance alternative materials is indispensable to achieve cost-effective, highly efficient water splitting process [32]. Momeni and Ghayeb [37] produced Fe/TNTs composites for water splitting applications with varying amounts of the iron source

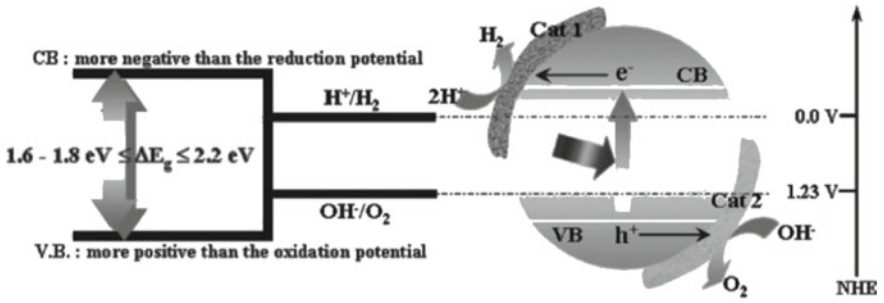

Fig. 6 The general principle of photocatalytic water splitting reactions. Reprinted with permission [35]

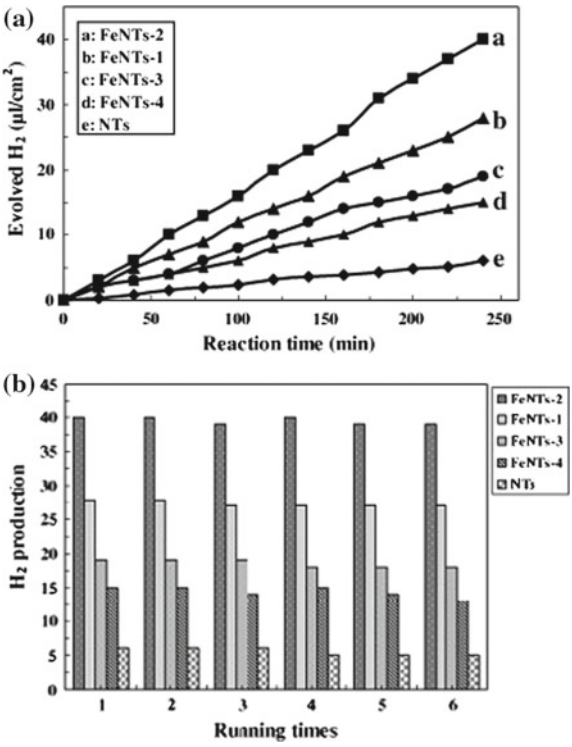

Fig. 7 **a** Photocatalytic H_2 production of different samples over irradiation, with applied external voltage [1.50 V (vs. Ag/AgCl)]. **b** H_2 evolution for different samples as a function of running times (reusability test of samples). Reprinted with permission [37]

potassium ferricyanide ($K_3Fe(CN)_6$), for which the ideal concentration was found to be 9 mM. Compared to undoped TNTs, the samples exhibited a red-shift of absorption edge and a band gap decrease, as well as a dramatic increase in photocurrent at the ideal Fe concentration. Regarding composite efficiency, Fig. 7a illustrates that the amount of H_2 evolved on the 9 mM Fe/TNTs sample (named FeNTs-2), after 240 min was more than 6,5 times the one verified on the undoped TiO_2 sample (NTs), and the hydrogen production showed no obvious decay after 6 continuous runs of photocatalytic reaction, as seen in Fig. 7b, thus proving the recyclability of the system.

3 Copper-Doped TiO_2

Exhibiting great potential for applications in the fields of solar energy conversion [38–40], photocatalytic hydrogen (H_2) production [32, 41, 42] and degradation of hazardous components [2, 43], earth-abundant and low-cost transitional metals such as cobalt (Co), nickel (Ni) and copper (Cu) [44, 45] have been successfully loaded on semiconductors in order to improve photocatalytic processes. According to Ran

et al. [32], applying such metals as cocatalysts promote charge separation due to the Schottky barrier formed at the metal/semiconductor interface.

Regarding solar water splitting, hydrogen not only is vital for many industrial processes but also is thought to be an attractive, clean energy vector when combined with efficient fuel cells. The overall photocatalytic water splitting reaction involves three major steps, those being light absorption by a semiconductor to generate electron-hole pairs, charge separation and migration to the surface of the semiconductor and finally surface reactions for H_2 or O_2 evolution [32] (Fig. 8). However, solar photocatalytic water splitting is still a challenging promise for sustainable H_2 production, mostly because the ideally described use of platinum (Pt) as cocatalyst endures a series of limitations linked to its high-cost and relatively low availability [32, 41].

In this context arises an increasing interest in the aforementioned transition metals, especially Cu species, for the narrow band-gap characteristic of both CuO and Cu_2O extends the photoresponse of TiO_2 into the visible light region [2, 38–40, 43, 46], making them a sustainable candidate for TiO_2 doping to enhance hydrogen production [44, 47]. On that note, Xu et al. [48] reported that CuO-loaded TiO_2 exhibited a photocatalytic H_2 production rate in methanol aqueous solution about 3 times higher than that of some Pt/TiO_2 electrodes (18,500 $\mu mol\, h^{-1}\, g^{-1}{}_{catalyst}$ to 6000 [49] and 6900 [50] $\mu mol\, h^{-1}\, g^{-1}{}_{catalyst}$, respectively). Furthermore, it was found that Cu-doping process does not influence the morphology of TiO_2 samples [43, 51], and different chemical states of Cu species, as well as their distribution ratio over

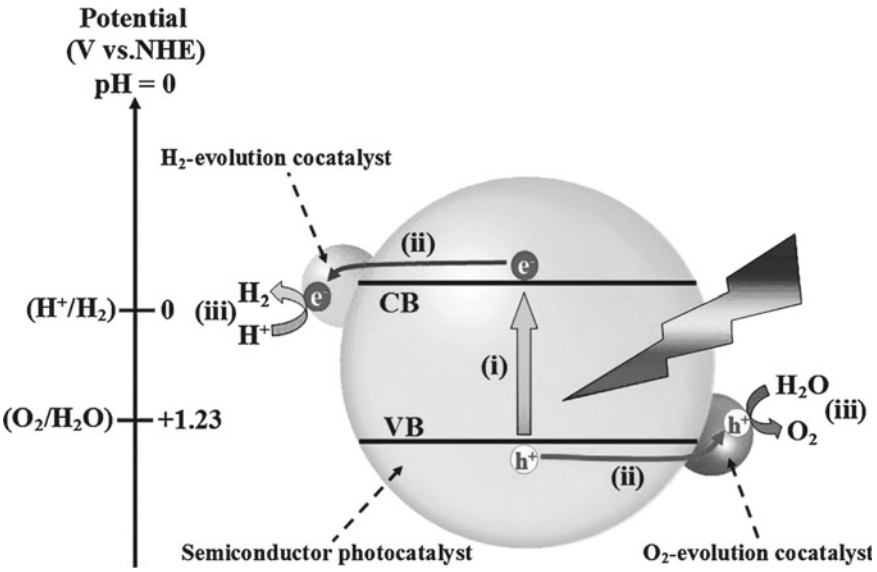

Fig. 8 Schematic illustration of photocatalytic water splitting over a semiconductor photocatalyst loaded with H_2^- and O_2^- evolution cocatalysts. Reprinted with permission [32]

TiO_2 notably influence H_2 production activities, with Cu species aggregated to its surface promoting charge transfer more efficiently than those in TiO_2 lattice [42].

The stability of the system is also to be observed, for leaching of non-metals is one of the main reasons for catalyst deactivation in liquid media [41]. Gombac et al. [41] tested copper leaching during and after photocatalytic reactions carried with a Cu/TiO_2 electrode both under reducing and oxidizing conditions, those being argon flow and inert atmosphere and exposure to air, respectively. Results indicated that under reducing conditions Cu leaching is marginal and, if operative, can be minimized by UV irradiation. On the other hand, dramatic leaching is observed under oxidized conditions.

Coupling Cu NPs with self-organized, highly ordered TiO_2 nanotube arrays (Cu/TNTs) creates an even more efficient opportunity to harvest sunlight when compared to randomly oriented TiO_2 nanoparticles [2]. Cu/TNTs heterojunction also favors the separation of photogenerated electron-hole pairs, ultimately improving photoelectrical conversion ability under solar light irradiation [40, 43]. Hua et al. [43] confirmed such aspect by varying deposition time of Cu NPs over TNTs, for which the increase in deposition time also meant an increase in the transient photocurrent response (Fig. 9). Moreover, uniformly dispersed Cu NPs ensured the electron migration by forming a strong interaction with TNTs, thereby improving charge transfer and separation.

In the same study, Hua et al. [43] evaluated the catalytic efficiency of Cu/TNTs electrodes for degrading of diclofenac (DCF), a non-steroidal anti-inflammatory drug vastly researched for its endocrine disrupting and adverse effects and also one of the most frequently detected pharmaceuticals in municipal wastewater [52]. Among the

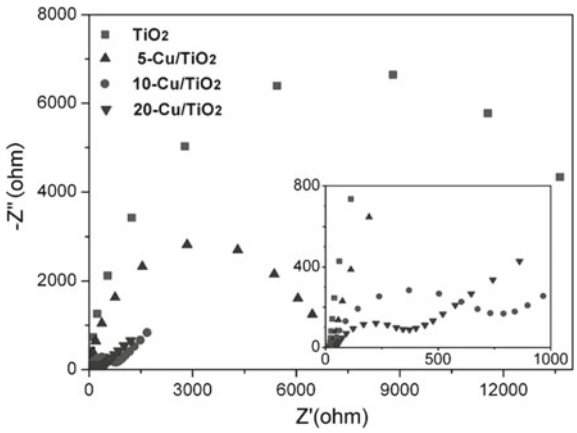

Fig. 9 Electrochemical impedance spectroscopy (EIS) spectra of Cu/TNTs electrodes, recorded at the open circuit potential under simulated solar light irradiation. The semicircle diameter of EIS, related to charge transfer resistance and separation efficiency at the contact interface between the electrode and electrolyte, was substantially decreased with increasing the deposition time, which could be attributed to Cu_2O and CuO improving the harvesting of visible light and reducing the transfer impedance of electrons. Reprinted with permission [43]

four processes tested, electrochemical (EC), direct photolysis (DP), photocatalysis (PC) and photoelectrocatalysis (PEC), the PEC process was found to be the most efficient with a DCF degradation efficiency of 71.9%, pointing to the important role played by an applied potential bias of 0.5 V in effectively separating electron-hole pairs and prolonging lifetime of the photogenerated charge carriers (Fig. 10).

Similar research utilizing the previously mentioned catalytic processes (EC, DP, PC, and PEC) was carried by Hou et al. [2] for 4-chlorophenol (4-CP) decomposition under UV light irradiation. As depicted in Fig. 11 the photocurrent density of the

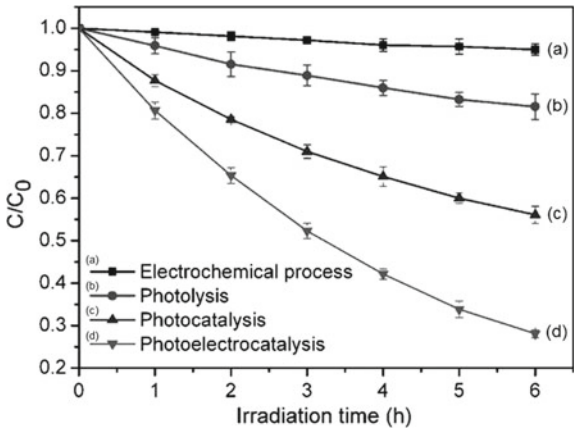

Fig. 10 Degrading DCF by electrochemical process (curve A), photolysis (curve B), photocatalysis (curve C) and photoelectrocatalysis (curve D) over Cu/TNTs electrode. Reprinted with permission [43]

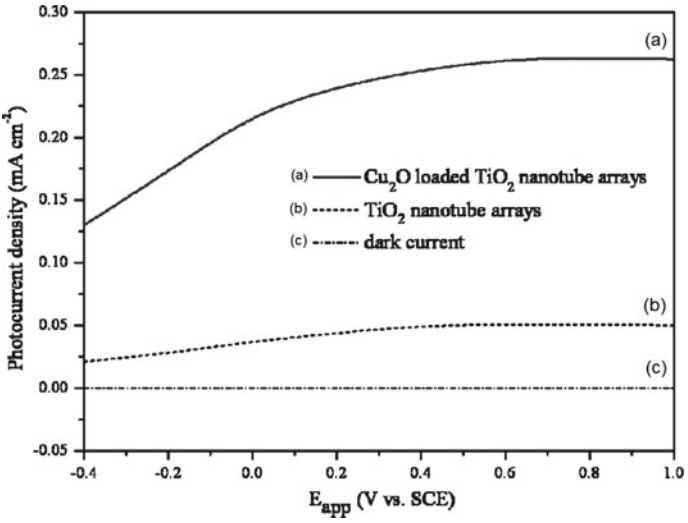

Fig. 11 Variation of photocurrent density versus bias potential (vs. SCE) in 0.01 M Na_2SO_4 solution for the Cu_2O-loaded TiO_2 nanotube array electrode and TiO_2 nanotube array electrode under Xe lamp (400–600 nm, 33 mW cm^{-2}) irradiation. Reprinted with permission [2]

Cu_2O/TNT electrode was measured to be more than 5 times the value for the non-loaded TNTs. Again, the PEC process utilizing a Cu_2O/TNT electrode was the fastest among the four alternatives, achieving nearly 100% of 4-CP degradation in 120 min, a value at least 20% higher than the one measured for the PEC process with a non-loaded TNT electrode (Fig. 12). Similarly, maximum photoconversion efficiency was observed at an applied bias of 0.1 V, corroborating the idea proposed by Hua et al. [43] that a potential bias inhibits the recombination of photogenerated electron-hole pairs.

Cu_2O appears yet in structures other than NPs. As an example, Yang et al. [46] incorporated both Cu^0 NPs on the inner walls (Fig. 13a) and Cu_2O nanowires onto the top surface of TNTs (Fig. 13b) for p-nitrophenol (PNP) degradation, creating an intercrossed network with extended absorption in the visible light range without blocking the nanotubes (Fig. 13c).

Used for drug, fungicide and dye manufacturing, the priority pollutant is generally degraded by strong oxidants only, thus impeding purification of PNP-contaminated wastewater due to its stability to chemical and biological degradation [53, 54]. However, the authors proved that under solar light PNP can be effectively degraded by the Cu_2O/TNT p-n junction network without the addition of oxidants, at a rate 2.3 times higher than the unmodified TiO_2 NTs (1.97 μg/min cm^2 versus 0.85 μg/min cm^2, respectively).

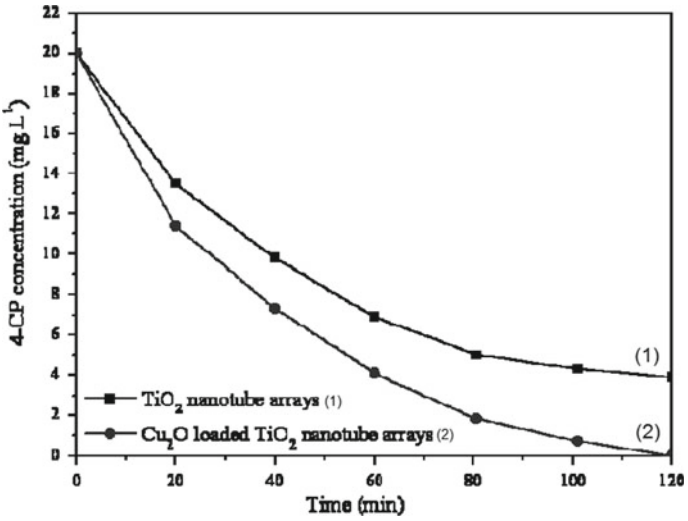

Fig. 12 Variation of 4-CP concentrations by photoelectrocatalytic (PEC) technology with TiO_2 nanotube array electrode and Cu_2O-loaded TiO_2 nanotube array electrode under UV light illumination (I_0 = 1.4 mW cm^{-2}, 0.2 V vs. SCE bias potential applied). Reprinted with permission [2]

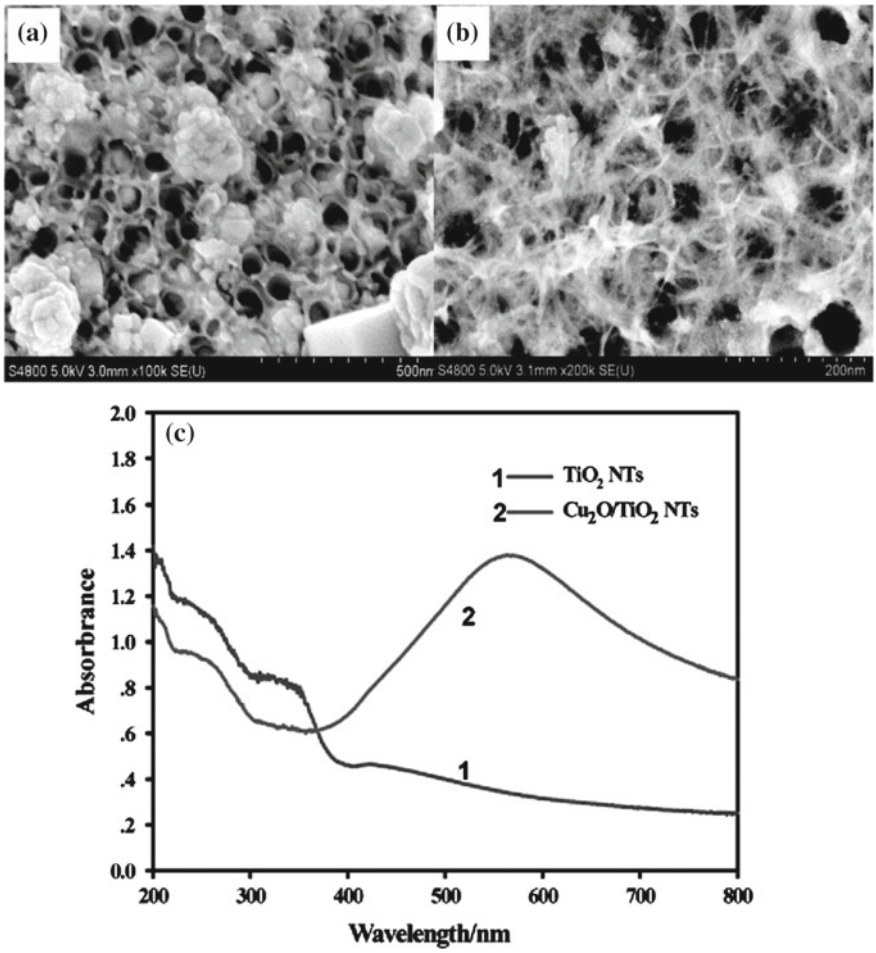

Fig. 13 SEM images of **a** Cu-loaded TiO_2 NTs and **b** Cu_2O ultrafine nanowires modified TiO_2 NTs. **c** UV-vis absorption spectra of TNTs (curve 1) and Cu_2O/TNTs (curve 2), demonstrating that the Cu_2O-modified TNTs have intense absorption in the visible light range. Reprinted with permission [46]

3.1 Silver/TiO_2 Nanostructures

The addition of nanostructured silver to titanium dioxide (Ag/TiO_2) has been thoroughly studied, mainly in terms of its photocatalytic properties [55–57]. Several studies [55, 58–60] demonstrate that silver is one of the most suitable materials for industrial application, due to the easy preparation and consequently low cost [58]. Because it is a noble metal, Ag presents characteristics that improve the photocatalytic activity of TiO_2 [61] as already mentioned (Fig. 14).

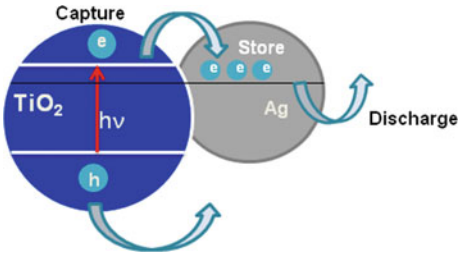

Fig. 14 Electron transfer mechanism in silver loaded TiO_2. Reprinted with permission [61]

Amongst the main properties directly linked to the addition of silver to the surface is the facility to dispose of photogenerated electrons on the TiO_2 surface, directly attached to the silver fermi energy being just below the conduction band of TiO_2, thus causing silver in this way function as a storage point of photogenerated load. Besides, the nanostructure of silver facilitates the photoabsorption process, due to the effects of SPR, which depend directly on the geometry and size of the nanostructures. Plasmon resonance effects can amplify the discharge effect for photoactive surfaces.

The Ag loaded TiO_2 (Ag/TiO_2), recently have been used in applications that aim pollutants and dyes degradation of wastewater. Seery [62] evaluated the rate of degradation of a model dye, rhodamine (R6G), and samples produced by different methods (irradiation and calcination) and the amount of silver doping. The author [62] relates that the degradation rate of the calcinated sample presented the most efficient catalytic properties (6–50% improvement in catalytic efficiency), that can be attributed to the silver is homogeneously dispersed throughout the material. The degradation rate of (R6G) oscillates among 0.06 min^{-1} for TiO_2 to 0.34 min^{-1} for 5 mol% $Ag–TiO_2$, which is attributed to the increasingly visible absorption capacity by Ag presence [62].

Concerning the pollutant materials, Li [63] explored the degradation of toluene with TiO_2 nanotube powder doped with Ag nanoparticles and compared the photocatalytic efficiency with commercial TiO_2 (P25, Degussa). The TiO_2 nanotubes were produced from Titanium foils with potenciostatic anodization method. The anodization was performed in a two-electrode configuration, where the Ti foil was used as a working electrode, and platinum foil as the counter electrode. The Ag-doped TiO_2 were prepared employing an incipient wetness impregnation method. The Ag/TiO_2 powder photocatalytic activity was measured through photo-oxidation of gaseous toluene. The results indicated that achieved efficiency for toluene degradation was 98% after 4 h reaction, under UV-light, these values were better than with pure TiO_2, Ag-doping P25 or P25 [63].

Another application that has been extensively studied using Ag/TiO_2 is water splitting, to generate gaseous H_2 as an alternative energy source. To enhance the process efficiency, Fan [64] produced highly ordered Fe^{3+}-doped TiO_2 nanotube arrays (Fe/TiO_2 NTs), then Ag nanoparticles were assembled in $Ag\text{-}Fe/TiO_2$ NTs. The material assembly with iron was prepared by electrochemical anodic oxidation

and the Ag was loaded by microwave-assisted chemical reduction. The author related that Ag-Fe/TiO_2 NTs showed higher UV-Vis light absorption and lower electron-hole recombination rate than pure TiO_2 (Fig. 15). The photocatalytic

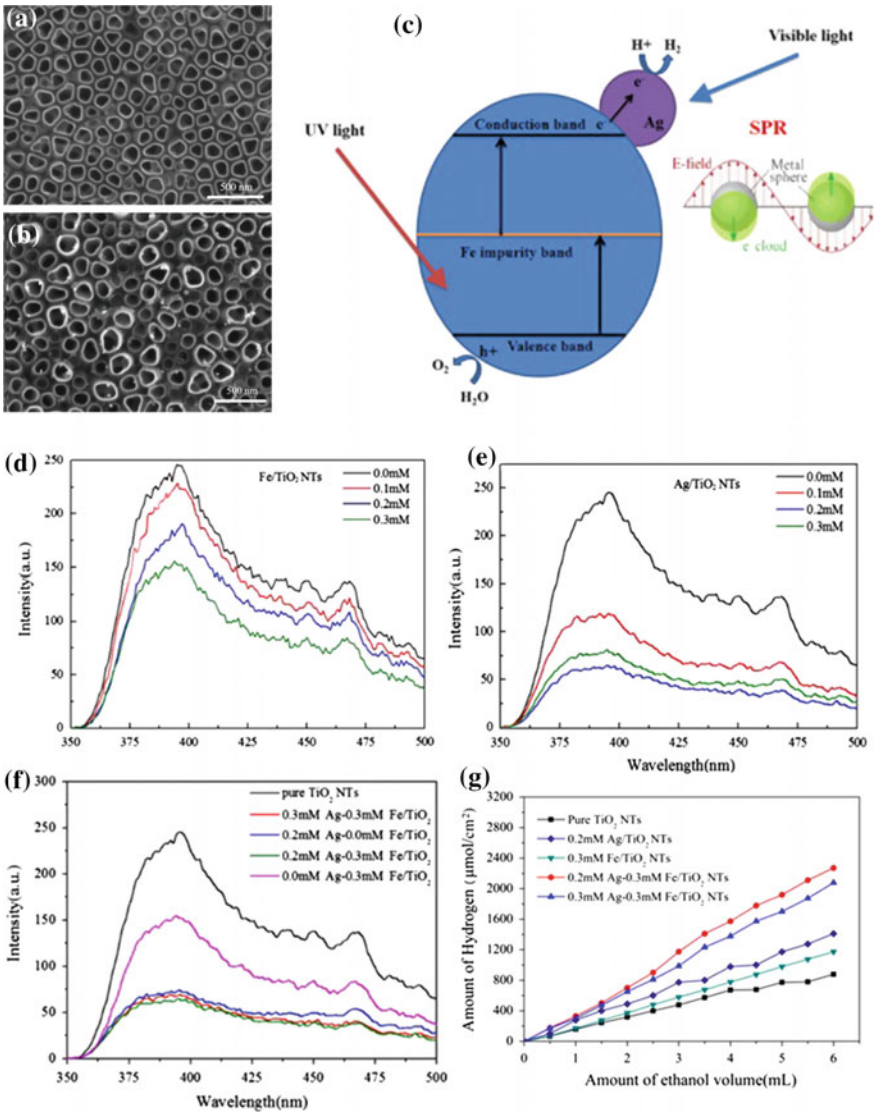

Fig. 15 **a** SEM images of pure TiO_2 NTs and **b** Fe doped and Ag NPs loaded on TiO_2 NT. **c** Mechanism of H_2 production by water splitting over Ag–Fe/TiO_2 NTs applying UV and visible light irradiation. **d** Photoluminescence spectra of TiO_2 NTs under the excitation of 250 nm Fe/TiO_2 NTs, **e** Ag/TiO_2 NTs and **f** Ag–Fe/TiO_2 NTs. **g** H_2 production by water splitting by TiO_2 catalysts. (*Ag/TiO_2–Ag-doped TiO_2). Reprinted with permission [64]

activity indicated a higher efficiency by 0.2 mM Ag-0.3 mM Fe/TiO_2 NTs samples. if compared with the pure TiO_2 catalyst. These results show the potential of photocatalytic material for energy and environment applications [64].

3.2 Gold

Gold is another noble metal that possesses singular electronic properties. Several researchers [65–67] relates that the presence of gold (Au) in nanoparticle form, or combined with other noble metals in TiO_2 supports, will improve the photocatalytic degradation of pollutants. In this regard, reports [68, 69], relate researches about the photocatalytic oxidation of pesticides and phenolic compounds applying TiO_2, furthermore, reviewed concerning the organic dyes degradation in effluents.

Sanabrina [66] has investigated the performance of Au and platinum (Pt) nanoparticles, and Au–Pt alloy on anodic TiO_2 nanotubes (TiO_2 NTs) for photocatalytic degradation. The materials were produced with a different method, that is, metal decoration intrinsically and extrinsically. The intrinsical decoration was obtained using a noble metal-containing titanium alloy for anodic tube growth, as the extrinsic decoration was realized by physical vapor deposition (PVD) method of the Ag and Pt on pure titania tubes (Fig. 16).

The results showed enhancement for decomposition of the model pollutant acid orange 7 (AO7) when the Au–Pt intrinsic decoration was evaluated, which can be attributed to the synergistic effect of both noble metals. This effect of Au- Pt intrinsic decoration has revealed to be a better option than the use of pure elements loaded on TiO_2 NTs. Sanabrina [66] relates the overall effect is due to the facilitated oxygen reduction reaction, which leads to higher production of reactive oxygen species on the conduction band, which provide an enhanced pollutant degradation rate [66].

Beyond the photocatalysis application, it is possible to cite the H_2 production using TiO_2 nanotubes (TiO_2 NTs) doped with Au. Choi [67] produced Au NP-decorated TiO_2 nanotube arrays (TNTs) to apply as photoelectrochemical (PEC) water splitting electrodes for H_2 production. To synthesize the TNTs, the author made use of a simple and low-cost method with two-step anodization process, and finally the deposition of a thin film of Au nanoparticles (Fig. 17) [67].

The TiO_2 NTs prepared using the two-step anodization process showed better photocurrent stability and efficiency. Furthermore, the Au presence on TNT array increases the photocurrent value in 67.2% to 1.02 mA/cm^2. The PEC process water splitting was enhanced and stabilized for charge separation and transport due to reduced cracking after second anodization and the annealing process [67].

Based on the context presented in this chapter, it is important to cite Paramasivam [70], that compared the photocatalytic activity of Au and Ag nanoparticles loaded TiO_2 nanotubes and the activity of the unloaded TiO_2 substrates. Paramasivam relates an enhancement of photocatalytic activity with TiO_2 nanotubular structures compared with a compact TiO_2 surface, which possesses higher performance due to SPR enhancement properties due to the presence of Au and Ag.

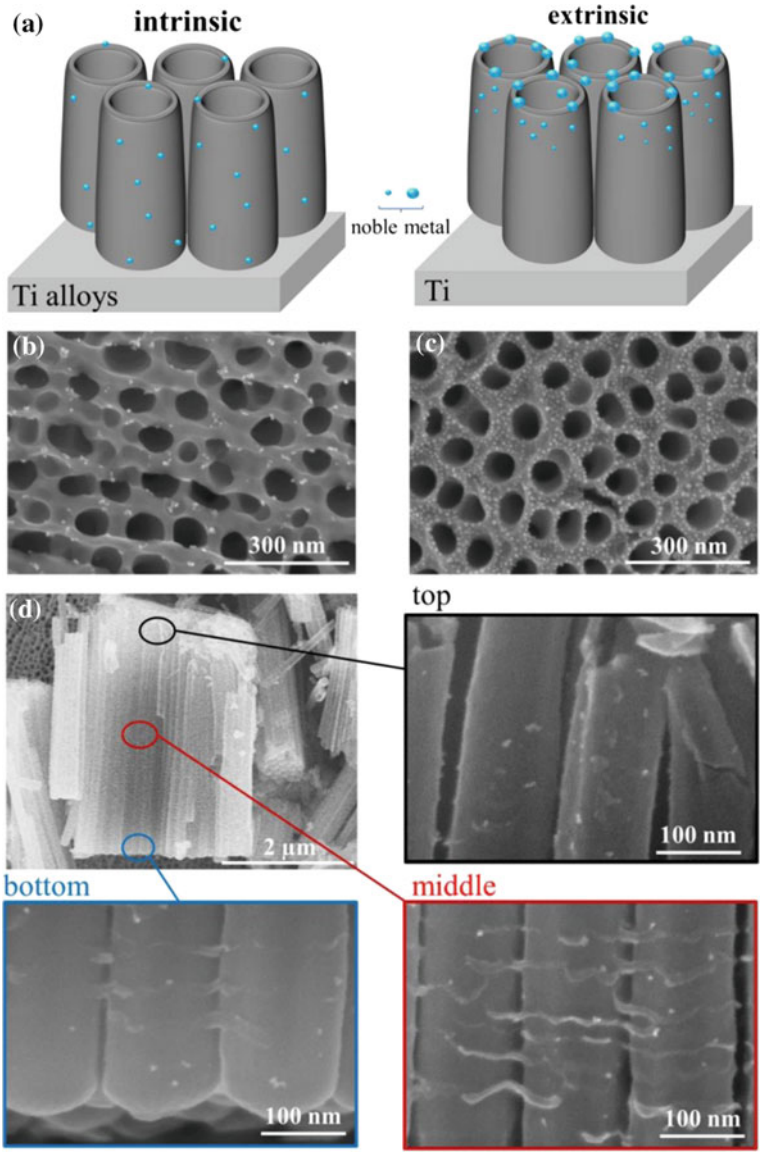

Fig. 16 **a** Representation of TiO_2 NTs intrinsically decorated by direct anodization of alloy (left) and extrinsically decorated by sputtering and dewetting a noble metal on the top of the NTs anodically growth on Ti foil (right); **b** top section of the NTs on TiAuPt alloy; **c** top section of the TiO_2 NTs with 1 nm of Au dewetted and **d** cross-section of the NTs on TiAuPt alloy with magnifications in the top, middle and bottom part identified by different colors black, blue and red. Reprinted with permission [66]

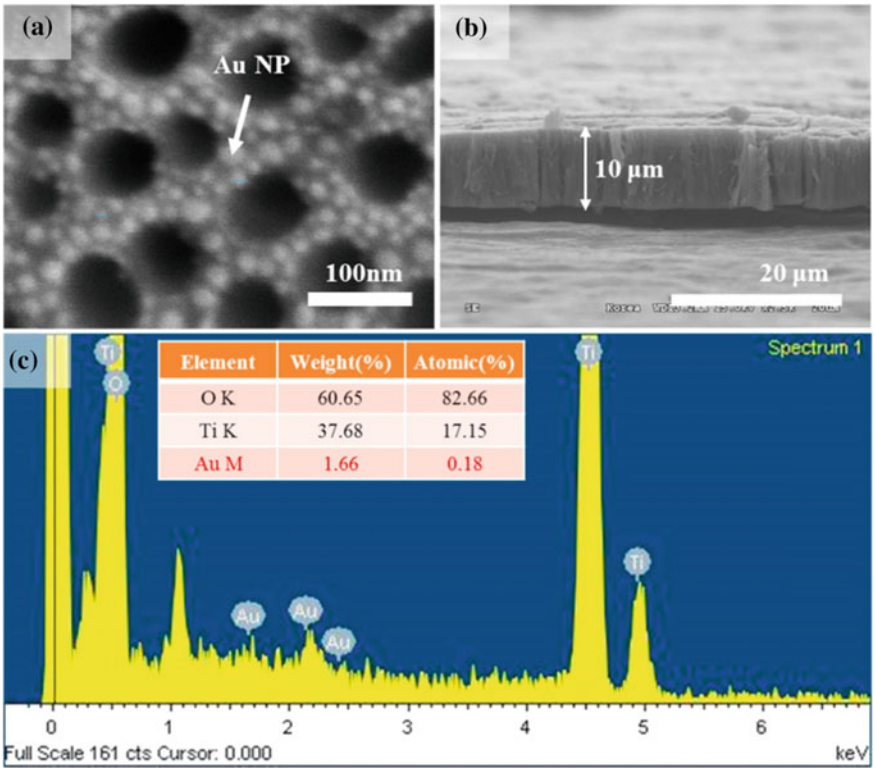

Fig. 17 SEM images of Au NP-decorated 2 nd anodized TNT arrays **a** top-view and **b** cross sectional view. **c** EDX analysis of Au NP-decorated 2 and anodized TNT arrays (TNT–Au NP-decorated TiO_2 nanotube). Reprinted with permission [67]

4 Conclusions

In summary, modifying TiO_2 with semiconductor materials, distinctly Fe and Cu ions, creates additional energy levels near the valence and conduction bands of TiO_2, thus minimizing the limitations associated with its large band gap via trapping of both electrons and holes. Consequently, it is highly recommended to dope TiO_2 with either Fe or Cu ions to obtain superior photocatalytic activity [6, 71]. Furthermore, the nanotubes loaded with Ag provide a doubled degradation when compared with pure nanotubes. The improvement of photocatalytic activity using Ag-TiO_2 can be explained considering the deposition method, which a thermal treatment step is recommended as an activation step, otherwise the addition of this metal may lead to decreased activity compared to pure TiO_2 NTs. Finally, the presence of the noble metal establish the formation of locally Schottky junctions with a high potential gradient, compared with TiO_2/electrolyte interface, established by Schottky barrier, which enables better charge tranfer between the materials. In view of the aforemen-

tioned results, it is possible to state that the addition of metallic structures, like Fe, Cu, Ag and Au, to TiO_2 NTs have a great potential to be used in photocatalytic reactions and water-splitting applications.

References

1. Zhang Y, Gu D, Zhu L, Wang B (2017) Highly ordered Fe^{3+}/TiO_2 nanotube arrays for efficient photocatalytic degradation of nitrobenzene. Appl Surf Sci 420:896–904. https://doi.org/10.1016/j.apsusc.2017.05.213
2. Hou Y, Li X, Zou X, Quan X, Chen G (2009) Photoeletrocatalytic activity of a Cu_2O-loaded self-organized highly oriented TiO_2 nanotube array electrode for 4-chlorophenol degradation. Environ Sci Technol 43:858–863. https://doi.org/10.1021/es802420u
3. Baker DR, Kamat PV (2009) Photosensitization of TiO_2 nanostructures with CdS quantum dots: particulate versus tubular support architectures. Adv Funct Mater 19:805–811. https://doi.org/10.1002/adfm.200801173
4. Teh CM, Mohamed AR (2011) Roles of titanium dioxide and ion-doped titanium dioxide on photocatalytic degradation of organic pollutants (phenolic compounds and dyes) in aqueous solutions. J Alloys Compd 509:1648–1660. https://doi.org/10.1016/j.jallcom.2010.10.181
5. Ambrus Z, Balázs N, Alapi T, Wittmann G, Sipos P, Dombi A, Mogyorósi K (2008) Synthesis structure and photocatalytic properties of Fe(III)-doped TiO_2 prepared from $TiCl_3$. Appl Catal B Environ 81:27–37. https://doi.org/10.1016/j.apcatb.2007.11.041
6. Choi W, Termin A, Hoffmann MR (1994) The role of metal ion dopants in quantum-sized TiO_2: correlation between photoreactivity and charge carrier recombination dynamics. J Phys Chem 98:13669–13679. https://doi.org/10.1021/j100102a038
7. Kraeutler B, Bard AJ (1978) Heterogeneous photocatalytic decomposition of saturated carboxylic acids on titanium dioxide powder. Decarboxylative route to alkanes. J Am Chem Soc 100:5985–5992. https://doi.org/10.1021/ja00487a001
8. Bard AJ (1979) Photoelectrochemistry and heterogeneous photo-catalysis at semiconductors. J Photochem 10:59–75. https://doi.org/10.1016/0047-2670(79)80037-4
9. Papp J, Soled S, Dwight K, Wold A (1994) Surface acidity and photocatalytic activity of and photocatalysts. Chem Mater 6:496–500. https://doi.org/10.1021/cm00040a026
10. Hoffmann MR, Martin ST, Choi W, Bahnemann DW (1995) Environmental applications of semiconductor photocatalysis. Chem Rev 95:69–96. https://doi.org/10.1021/cr00033a004
11. Zhang ZB, Wang CC, Zakaria R, Ying JY (1998) Role of particle size in nanocrystalline TiO_2-based photocatalysts. J Phys Chem Biol 102:10871–10878. https://doi.org/10.1021/jp982948+
12. Wang CY, Bahnemann DW, Dohrmann JK (2000) A novel preparation of iron-doped TiO_2 nanoparticles with enhanced photocatalytic activity. Chem Commun 0:1539–1540. https://doi.org/10.1039/b002988m
13. Adán C, Bahamonde A, Fernández-García M, Martínez-Arias A (2007) Photocatalytic degradation of ethidium bromide over titania in aqueous solutions. Appl Catal B Environ 72:11–17. https://doi.org/10.1016/j.apcatb.2006.09.018
14. Serpone N, Lawless D, Disdier J, Herrmann JM (1994) Spectroscopic, photoconductivity, and photocatalytic studies of TiO_2 colloids: naked and with the lattice doped with Cr^{3+}, Fe^{3+}, and V^{5+} cations. Langmuir 10:643–652. https://doi.org/10.1021/la00015a010
15. Zhu J, Zheng W, He B, Zhang J, Anpo M (2004) Characterization of Fe–TiO_2 photocatalysts synthesized by hydrothermal method and their photocatalytic reactivity for photodegradation of XRG dye diluted in water. J Mol Catal A Chem 216:35–43. https://doi.org/10.1016/j.molcata.2004.01.008
16. Zhu J, Chen F, Zhang J, Chen H, Anpo M (2006) Fe^{3+}–TiO_2 photocatalysts prepared by combining sol-gel method with hydrothermal treatment and their characterization. J Photochem Photobiol A Chem 180:196–204. https://doi.org/10.1016/j.jphotochem.2005.10.017

17. Wang XH, Li JG, Kamiyama H, Moriyoshi Y, Ishigaki T (2006) Wavelength-sensitive photocatalytic degradation of methyl orange in aqueous suspension over Iron(III)-doped TiO_2 nanopowders under UV and visible light irradiation. J Phys Chem B 110:6804–6809. https://doi.org/10.1021/jp060082z
18. Yu H, Irie H, Shimodaira Y, Hosogi Y, Kuroda Y, Miyauchi M, Hashimoto K (2010) An efficient visible-light-sensitive Fe(III)-grafted TiO_2 photocatalyst. J Phys Chem C 114:16481–16487. https://doi.org/10.1021/jp1071956
19. Asiltürk M, Sayilkan F, Arpaç E (2009) Effect of Fe^{3+} ion doping to TiO_2 on the photocatalytic degradation of Malachite Green dye under UV and vis-irradiation. J Photochem Photobiol A Chem 203:64–71. https://doi.org/10.1016/j.jphotochem.2008.12.021
20. Frandsen C, Bahl CRH, Lebech B, Lefmann K, Kuhn LT, Keller L, Andersen NH, Zimmermann MV, Johnson E, Klausen SN, Mørup S (2005) Oriented attachment and exchange coupling of $\alpha-Fe_2O_3$ nanoparticles. Phys Rev B Condens Matter Mater Phys 72:214406. https://doi.org/10.1103/physrevb.72.214406
21. Spray RL, McDonald KJ, Choi KS (2011) Enhancing photoresponse of nanoparticulate α-Fe_2O_3 electrodes by surface composition tuning. J Phys Chem C 115:3497–3506. https://doi.org/10.1021/jp1093433
22. Xie S, Ouyang K, Lao Y, He P, Wang Q (2017) Heterostructured $ZnFe_2O_4/TiO_2$ nanotube arrays with remarkable visible-light photoelectrocatalytic performance and stability. J Colloid Interface Sci 493:198–205. https://doi.org/10.1016/J.JCIS.2017.01.023
23. Cong Y, Li Z, Zhang Y, Wang Q, Xu Q (2012) Synthesis of α-Fe_2O_3/TiO_2 nanotube arrays for photoelectro-Fenton degradation of phenol. Chem Eng J 191:356–363. https://doi.org/10.1016/j.cej.2012.03.031
24. Yang X, Zou R, Huo F, Cai D, Xiao D (2009) Preparation and characterization of $Ti/SnO_2–Sb_2O_3–Nb_2O_5/PbO_2$ thin film as electrode material for the degradation of phenol. J Hazard Mater 164:367–373. https://doi.org/10.1016/j.jhazmat.2008.08.010
25. Li XY, Cui YH, Feng YJ, Xie ZM, Gu JD (2005) Reaction pathways and mechanisms of the electrochemical degradation of phenol on different electrodes. Water Res 39:1972–1981. https://doi.org/10.1016/j.watres.2005.02.021
26. Shihong X, Daolun F, Wenfeng S (2009) Preparations and photocatalytic properties of visible-light-active zinc ferrite-doped TiO_2 photocatalyst. J Phys Chem C 113:2463–2467. https://doi.org/10.1021/jp806704y
27. Hou Y, Li XY, Zhao QD, Quan X, Chen GH (2010) Electrochemical method for synthesis of a $ZnFe_2O_4/TiO_2$ composite nanotube array modified electrode with enhanced photoelectrochemical activity. Adv Funct Mater 20:2165–2174. https://doi.org/10.1002/adfm.200902390
28. Theurich J, Lindner M, Bahnemann DW (1996) Photocatalytic degradation of 4-Chlorophenol in aerated aqueous titanium dioxide suspensions: a kinetic and mechanistic study. Langmuir 12:6368–6376. https://doi.org/10.1021/la960228t
29. Venkatachalam N, Palanichamy M, Murugesan V (2007) Sol-gel preparation and characterization of alkaline earth metal doped nano TiO_2: efficient photocatalytic degradation of 4-chlorophenol. J Mol Catal A Chem 273:177–185. https://doi.org/10.1016/j.molcata.2007.03.077
30. Fujishima A, Honda K (1972) Electrochemical photolysis of water at a semiconductor electrode. Nature 238:37–38. https://doi.org/10.1038/238037a0
31. Momeni MM, Ghayeb Y, Davarzadeh M (2015) Single-step electrochemical anodization for synthesis of hierarchical $WO_3–TiO_2$ nanotube arrays on titanium foil as a good photoanode for water splitting with visible light. J Electroanal Chem 739:149–155. https://doi.org/10.1016/j.jelechem.2014.12.030
32. Ran J, Zhang J, Yu J, Jaroniec M, Qiao SZ (2014) Earth-abundant cocatalysts for semiconductor-based photocatalytic water splitting. Chem Soc Rev 43:7787–7812. https://doi.org/10.1039/c3cs60425j
33. Ahmad H, Kamarudin SK, Minggu LJ, Kassim M (2015) Hydrogen from photo-catalytic water splitting process: a review. Renew Sustain Energy Rev 43:599–610. https://doi.org/10.1016/j.rser.2014.10.101

34. Grätzel M (2001) Photoelectrochemical cells. Nature 414:338–344. https://doi.org/10.1038/35104607
35. Jang JS, Kim HG, Lee JS (2012) Heterojunction semiconductors: a strategy to develop efficient photocatalytic materials for visible light water splitting. Catal Today 185:270–277. https://doi.org/10.1016/j.cattod.2011.07.008
36. Meher LC, Vidya Sagar D, Naik SN (2006) Technical aspects of biodiesel production by transesterification—a review. Renew Sustain Energy Rev 10:248–268. https://doi.org/10.1016/j.rser.2004.09.002
37. Momeni MM, Ghayeb Y (2015) Fabrication, characterization and photoelectrochemical behavior of Fe–TiO_2 nanotubes composite photoanodes for solar water splitting. J Electroanal Chem 751:43–48. https://doi.org/10.1016/j.jelechem.2015.05.035
38. Siripala W, Ivanovskaya A, Jaramillo TF, Baeck SH, McFarland EW (2003) A Cu_2O/TiO_2 heterojunction thin film cathode for photoelectrocatalysis. Sol Energy Mater Sol Cells 77:229–237. https://doi.org/10.1016/S0927-0248(02)00343-4
39. Lu C, Qi L, Yang J, Wang X, Zhang D, Xie J, Ma J (2005) One-pot synthesis of octahedral Cu_2O nanocages via a catalytic solution route. Adv Mater 17:2562–2567. https://doi.org/10.1002/adma.200501128
40. Wang J, Ji G, Liu Y, Gondal MA, Chang X (2014) Cu_2O/TiO_2 heterostructure nanotube arrays prepared by an electrodeposition method exhibiting enhanced photocatalytic activity for CO_2 reduction to methanol. Catal Commun 46:17–21. https://doi.org/10.1016/j.catcom.2013.11.011
41. Gombac V, Sordelli L, Montini T, Delgado JJ, Adamski A, Adami G, Cargnello M, Bernai S, Fornasiero P (2010) CuO_x-TiO_2 photocatalysts for H_2 production from ethanol and glycerol solutions. J Phys Chem A 114:3916–3925. https://doi.org/10.1021/jp907242q
42. Xu S, Ng J, Zhang X, Bai H, Sun DD (2010) Fabrication and comparison of highly efficient Cu incorporated TiO_2 photocatalyst for hydrogen generation from water. Int J Hydrogen Energy 35:5254–5261. https://doi.org/10.1016/j.ijhydene.2010.02.129
43. Hua Z, Dai Z, Bai X, Ye Z, Wang P, Gu H, Huang X (2016) Copper nanoparticles sensitized TiO_2 nanotube arrays electrode with enhanced photoelectrocatalytic activity for diclofenac degradation. Chem Eng J 283:514–523. https://doi.org/10.1016/j.cej.2015.07.072
44. Wu NL, Lee MS (2004) Enhanced TiO_2 photocatalysis by Cu in hydrogen production from aqueous methanol solution. Int J Hydrogen Energy 29:1601–1605. https://doi.org/10.1016/j.ijhydene.2004.02.013
45. Foo WJ, Zhang C, Ho GW (2013) Non-noble metal Cu-loaded TiO_2 for enhanced photocatalytic H_2 production. Nanoscale. 5:759–764. https://doi.org/10.1039/c2nr33004k
46. Yang L, Luo S, Li Y, Xiao Y, Kang Q, Cai Q (2010) High efficient photocatalytic degradation of p-Nitrophenol on a unique Cu_2O/TiO_2 p-n heterojunction network catalyst. Environ Sci Technol 44:7641–7646. https://doi.org/10.1021/es101711k
47. Sakata Y, Yamamoto T, Okazaki T, Imamura H, Tsuchiya S (1998) Generation of visible light response on the photocatalyst of a copper ion containing TiO_2. Chem Lett 27:1253–1254. https://doi.org/10.1246/cl.1998.1253
48. Xu S, Sun DD (2009) Significant improvement of photocatalytic hydrogen generation rate over TiO_2 with deposited CuO. Int J Hydrogen Energy 34:6096–6104. https://doi.org/10.1016/j.ijhydene.2009.05.119
49. Yi H, Peng T, Ke D, Ke D, Zan L, Yan C (2008) Photocatalytic H_2 production from methanol aqueous solution over titania nanoparticles with mesostructures. Int J Hydrogen Energy 33:672–678. https://doi.org/10.1016/J.IJHYDENE.2007.10.034
50. Sreethawong T, Puangpetch T, Chavadej S, Yoshikawa S (2007) Quantifying influence of operational parameters on photocatalytic H_2 evolution over Pt-loaded nanocrystalline mesoporous TiO_2 prepared by single-step sol-gel process with surfactant template. J Power Sources 165:861–869. https://doi.org/10.1016/J.JPOWSOUR.2006.12.050
51. Momeni MM, Ghayeb Y, Ghonchegi Z (2015) Fabrication and characterization of copper doped TiO_2 nanotube arrays by in situ electrochemical method as efficient visible-light photocatalyst. Ceram Int 41:8735–8741. https://doi.org/10.1016/j.ceramint.2015.03.094

52. Hartmann J, Bartels P, Mau U, Witter M, Tümpling WV, Hofmann J, Nietzschmann E (2008) Degradation of the drug diclofenac in water by sonolysis in presence of catalysts. Chemosphere 70:453–461. https://doi.org/10.1016/j.chemosphere.2007.06.063
53. Yi S, Zhuang WQ, Wu B, Tay STL, Tay JH (2006) Biodegradation of p-nitrophenol by aerobic granules in a sequencing batch reactor. Environ Sci Technol 40:2396–2401. https://doi.org/10.1021/es0517771
54. Labana S, Pandey G, Paul D, Sharma NK, Basu A, Jain RK (2005) Pot and field studies on bioremediation of p-Nitrophenol contaminated soil using arthrobacter protophormiae RKJ100. Environ Sci Technol 39:3330–3337. https://doi.org/10.1021/es0489801
55. Daghrir R, Drogui P, Robert D (2013) Modified TiO_2 for environmental photocatalytic applications: a review. Ind Eng Chem Res 52:3581–3599. https://doi.org/10.1021/ie303468t
56. He C, Yu Y, Hu X (2002) Influence of silver doping on the photocatalytic activity of titania films. Appl Surf Sci 200:239–247. https://doi.org/10.1016/s0169-4332(02)00927-3
57. Hajjaji A, Elabidi M, Trabelsi K, Assadi AA, Bessais B, Rtimi S (2018) Bacterial adhesion and inactivation on Ag decorated TiO_2-nanotubes under visible light: effect of the nanotubes geometry on the photocatalytic activity. Colloids Surf B Biointer 170:92–98. https://doi.org/10.1016/j.colsurfb.2018.06.005
58. Sun L, Li J, Wang C, Li S, Lai Y, Chen H, Lin C (2009) Ultrasound aided photochemical synthesis of Ag loaded TiO_2 nanotube arrays to enhance photocatalytic activity. J Hazard Mater 171:1045–1050. https://doi.org/10.1016/j.jhazmat.2009.06.115
59. Roy P, Berger S, Schmuki P (2011) TiO_2 nanotubes: synthesis and applications. Angew Chemie Int Ed 50:2904–2939. https://doi.org/10.1002/anie.201001374
60. Zhang J, Li S, Ding H, Li Q, Wang B, Wang X, Wang H (2014) Transfer and assembly of large-area TiO_2 nanotube arrays onto conductive glass for dye sensitized solar cells. J Power Sources 247:807–812. https://doi.org/10.1016/J.JPOWSOUR.2013.08.124
61. Etacheri V, Di Valentin C, Schneider J, Bahnemann D, Pillai SC (2015) Visible-light activation of TiO_2 photocatalysts: advances in theory and experiments. J Photochem Photobiol C Photochem Rev 25:1–29. https://doi.org/10.1016/j.jphotochemrev.2015.08.003
62. Seery M, George R, Pillai S, Floris P (2007) Silver doped titanium dioxide nanomaterials for enhanced visible-light photocatalysis. J Photochem Photobiol A 189:258–263. https://doi.org/10.1016/j.jphotochem.2007.02.010
63. Li X, Zou X, Qu Z, Zhao Q, Wang L (2011) Photocatalytic degradation of gaseous toluene over Ag-doping TiO_2 nanotube powder prepared by anodization coupled with impregnation method. Chemosphere 83:674–679. https://doi.org/10.1016/j.chemosphere.2011.02.043
64. Fan X, Fan J, Hu X, Liu E, Kang L, Tang C, Ma Y, Wu H, Li Y (2014) Preparation and characterization of Ag deposited and Fe doped TiO_2 nanotube arrays for photocatalytic hydrogen production by water splitting. Ceram Int 40:15907–15917. https://doi.org/10.1016/j.ceramint.2014.07.119
65. Zhang G, Miao H, Hu X, Mu J, Liu X, Han T, Fan J, Liu E, Yin Y, Wan J (2017) A facile strategy to fabricate Au/TiO_2 nanotubes photoelectrode with excellent photoelectrocatalytic properties. Appl Surf Sci 391:345–352. https://doi.org/10.1016/j.apsusc.2016.03.042
66. Sanabria-Arenas BE, Mazare A, Yoo J, Nguyen NT, Hejazi S, Bian H, Diamanti MV, Pedeferri MP, Schmuki P (2018) Intrinsic AuPt-alloy particles decorated on TiO_2 nanotubes provide enhanced photocatalytic degradation. Electrochim Acta 292:865–870. https://doi.org/10.1016/j.electacta.2018.09.206
67. Choi J-Y, Hoon Sung Y, Choi H-J, Doo Kim Y, Huh D, Lee H (2017) Fabrication of Au nanoparticle-decorated TiO_2 nanotube arrays for stable photoelectrochemical water splitting by two-step anodization. Ceram Int 43:14063–14067. https://doi.org/10.1016/j.ceramint.2017.07.141
68. Ahmed S, Rasul MG, Brown R, Hashib MA (2011) Influence of parameters on the heterogeneous photocatalytic degradation of pesticides and phenolic contaminants in wastewater: a short review. J Environ Manage 92:311–330. https://doi.org/10.1016/j.jenvman.2010.08.028

69. Ayati A, Ahmadpour A, Bamoharram FF, Tanhaei B, Mänttäri M, Sillanpää M (2014) A review on catalytic applications of Au/TiO_2 nanoparticles in the removal of water pollutant. Chemosphere 107:163–174. https://doi.org/10.1016/j.chemosphere.2014.01.040
70. Paramasivam I, Macak JM, Schmuki P (2007) Photocatalytic activity of TiO_2 nanotube layers loaded with Ag and Au nanoparticles. Electrochem Commun 10:71–75. https://doi.org/10.1016/j.elecom.2007.11.001
71. Litter MI (1999) Heterogeneous photocatalysis: transition metal ions in photocatalytic systems. Appl Catal B Environ 23:89–114. https://doi.org/10.1016/S0926-3373(99)00069-7